

Topological photonic states in one-dimensional dimerized ultracold atomic chains

B. X. Wang and C. Y. Zhao*

Institute of Engineering Thermophysics, Shanghai Jiao Tong University, Shanghai, 200240, China

(Dated: November 29, 2022)

The area of topological photonics attracts growing attention in the recent years. Herein, we theoretically and numerically study the topological optical states in one-dimensional (1D) dimerized ultracold atomic chains, as an analogy of the Su-Schrieffer-Heeger (SSH) model. We analytically calculate the band-structure and Zak phase for such chains beyond the tight-binding approximation. We find the 1D dimerized chain supports nontrivial topological states for dimerization parameter $\beta > 0.5$. Our findings are further corroborated by analyzing the eigenmode distribution and inverse participation ratio (IPR). The ultra strong scattering cross section and ultra-narrow linewidth of a single cold atom allow us to observe in more detail about topological states than in conventional systems, such as the frequency shift with respect to the single-atom resonance and the largely tunable bandgap. We also reveal that such topological edge states are robust under high-degree disorder and even enhanced by the disorder-induced Anderson localization. These topological photonic modes provide an efficient interface between light and matter.

The area of topological photonics attracts growing attention in the last decade [1, 2]. Specially designed topological photonic systems are able to create topologically protected optical states, which can propagate unidirectionally without any backscattering processes, even in the presence of disorder and impurities [1, 2]. Such systems show promising applications in novel photonic devices, such as unidirectional waveguides [3], optical isolators [4] as well as topological lasers [5]. Among them, one-dimensional (1D) and quasi-1D topological photonic systems, for instance, plasmonic nanoparticle chains [6, 7], lattices of optical waveguides [8] and arrays of dielectric resonators [3, 9] have received intense investigation due to their simplicity of fabrication and abilities of guiding and confining light. The simplest type of one-dimensional photonic systems with remarkable topological features is based on a photonic analogy of the Su-Schrieffer-Heeger (SSH) model describing dimerized chains [3, 6–8, 10], which was originally proposed in the electronic context. In fact, such topological photonic systems can be also realized through ultracold atoms. Nowadays, the techniques of optical lattices [11–13] and optical tweezers [14] are able to accurately manipulate the positions of ultracold atoms [15]. 1D and 2D arrays of ultracold atoms with near-unity perfect filling factor in a large scale (up to 50 atoms) can be fabricated [12, 13]. Regarding the very high resonant scattering cross section ($\sim \lambda_0^2$ where λ_0 is the wavelength of driving light) of a single ultracold atom, such ultracold atom arrays offer people an excellent platform for achieving strong light-matter interaction. The ultra-narrow linewidth of cold atoms compared to conventional optical scatterers also provides more fine observations about topological states than conventional systems.

In this paper, we propose one-dimensional dimerized ultracold atomic chains as a setup for the SSH model to study the topological edge states of light. Since for electromagnetic (EM) waves the retardation effect should be

included beyond the conventional nearest-neighbor approximation for electrons, especially the lattice period is larger than or comparable with the wavelength [7, 16], here based on a full-wave treatment, we analytically calculate the band-structures and Zak phases to classify the band topology of infinite dimerized cold atomic chains with different dimerized parameters. We find topologically protected states at the edges of topologically nontrivial dimerized chains as well as at the interface between chains with different Zak phases. We also reveal such topological states are robust under a high-degree disorder and even enhanced by the disorder-induced Anderson localization.

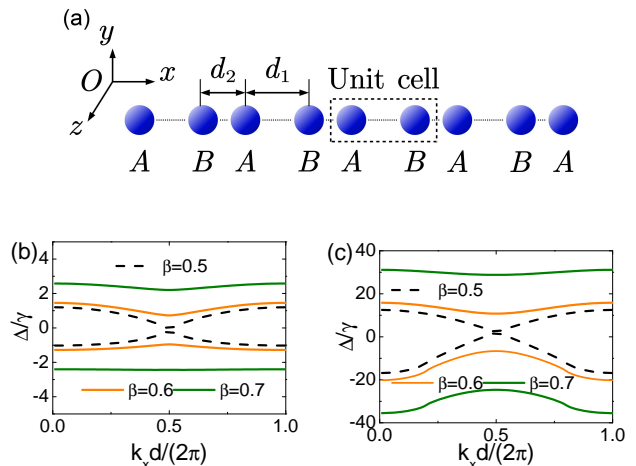


FIG. 1. (a) Schematic of the dimerized ultracold atomic chain. The atoms are identical and each sublattice with different lattice constants are denoted by A and B respectively. The inequivalent atom spacings are represented by d_1 and d_2 . (b) Band-structure of a dimerized chain with $d = d_1 + d_2 = 0.5\lambda_0$ for different dimerization parameter β . Here $\Delta = \omega - \omega_0$ stands for detuning, and $\lambda_0 = \omega_0/c$ is the wavelength at single-atom resonance. (c) The same as that in (b) but with $d = d_1 + d_2 = 0.2\lambda_0$.

The schematic of a dimerized, ultracold, and two-level atomic chain is shown in Fig. 1a, where the dimerization is introduced by using inequivalent spacings, $d_1 \neq d_2$, between two sublattices, denoted by A and B respectively. The overall period is then $d = d_1 + d_2$. Such dimerization leads to different ‘‘hopping’’ rates of photons in different directions. In the absence of nonlinear effects and Zeeman degeneracy of hyperfine sublevels as well as other internal quantum effects, for example, Sr atoms in the low excitation limit [17], the EM response of such two-level atomic chain is described by the coupled-dipole model [18, 19]:

$$\mathbf{p}_j(\omega) = -\alpha(\omega) \left[\mathbf{E}_{\text{inc}}(\mathbf{r}_j) + \frac{\omega^2}{c^2} \sum_{i=1, i \neq j}^{\infty} \mathbf{G}_0(\mathbf{r}_j, \mathbf{r}_i) \mathbf{p}_i \right], \quad (1)$$

where ω is the angular frequency of the driving field, c is the speed of light in vacuum. $\mathbf{E}_{\text{inc}}(\mathbf{r})$ is the external incident field and $\mathbf{p}_j(\omega)$ is the excited dipole moment of the i -th atom. $\mathbf{G}_0(\mathbf{r}_j, \mathbf{r}_i)$ is the free-space dyadic Greens function describing the propagation of field emitting from the i -th atom to j -th atom. The polarizability $\alpha(\omega)$ of an individual two-level atom is [20]

$$\alpha(\omega) = -\frac{6\pi c^3}{\omega^3} \frac{\gamma/2}{\omega - \omega_0 + i\gamma/2}, \quad (2)$$

where ω_0 is the resonance frequency of dipole transition and γ is the line-width. For 1D chains, there are two transverse (electric field orthogonal to the chain) and one longitudinal (electric field parallel to the chain) mode [21]. Here we only consider the longitudinal mode, whose dispersion relation with respect to the Bloch wavenumber along x -axis, k_x , is solved from the following eigenvalue problem derived from Eq. (1) with no incident field:

$$\frac{\omega^2}{c^2} \begin{pmatrix} a_{11}(k_x) & a_{12}(k_x) \\ a_{21}(k_x) & a_{22}(k_x) \end{pmatrix} \begin{pmatrix} p_A \\ p_B \end{pmatrix} = \alpha^{-1} \begin{pmatrix} p_A \\ p_B \end{pmatrix}, \quad (3)$$

where the diagonal elements are $a_{11}(k_x) = a_{22}(k_x) = \sum_{n=\text{even}, n \neq 0} G_{0,xx}(nd/2) \exp(ik_x nd/2)$, and the off-diagonal elements are $a_{12}(k_x) = \sum_{n=\text{odd}} G_{0,xx}((n-1)d/2 + d_1) \exp(ik_x((n-1)d/2))$ and $a_{21}(k_x) = \sum_{n=\text{even}} G_{0,xx}(nd/2 - d_1) \exp(ik_x(nd/2))$, where $G_{0,xx}(x) = -2 \left[\frac{i}{k|x|} - \frac{1}{(k|x|)^2} \right] \frac{\exp(ik|x|)}{4\pi|x|}$. Here the matrix elements are not unique, which are chosen such that it fulfills $a_{ij}(k_x + 2\pi/d) = a_{ij}(k_x + 2\pi/d)$, i.e., using the periodic gauge [6]. Such matrix can be regarded as playing the role of Hamiltonian for the photonic modes. Analytical calculation of the dispersion relation needs the aid of the Lerch transcendent [16]. The calculated bulk band-structures for $\beta = 0.5, 0.6, 0.7$ (The band-structures for $\beta = 0.3$ and $\beta = 0.4$ are the same as those for $\beta = 0.7$ and $\beta = 0.6$, respectively.) are shown in Figs. 1b (for $d = 0.5\lambda_0$) and 1c (for $d = 0.2\lambda_0$), where $\beta = d_1/d$ is the dimerization parameter. It is observed

that for $\beta \neq 0.5$, bandgaps are opened in both cases, while a smaller period leads to a wider bandgap. This is due to that the near-field dipole-dipole interactions between atoms can give rise to very strong frequency shift [22].

In analogy to the Berry phase, the Zak phase is able to determine the topology of bulk band-structure for 1D systems [6, 7, 16, 23]. Moreover, according to bulk-boundary correspondence, it also determines the existence of edge states [1]. For the non-Hermitian eigenvalue problem in Eq. (3), the Zak phase is obtained from the relative phase difference of p_A and p_B as [6, 7, 16, 23]

$$\gamma = \phi(\pi/d) - \phi(0), \quad (4)$$

where $\phi(k_x)$ is the relative phase difference between p_A and p_B for momentum k_x by solving the eigenvector of the matrix in Eq. (3). In Figs. 2a and 2b, we show $\phi(k_x)$ as a function of k_x for $d = 0.5\lambda_0$ and $d = 0.2\lambda_0$ respectively for the lower band. In both cases, it is found that for $\beta > 0.5$, the Zak phase is π (modulo 2π) while for $\beta < 0.5$ it is 0 (modulo 2π). $\beta = 0.5$ corresponds to a topological transition from topological trivial phase to a topological nontrivial phase.

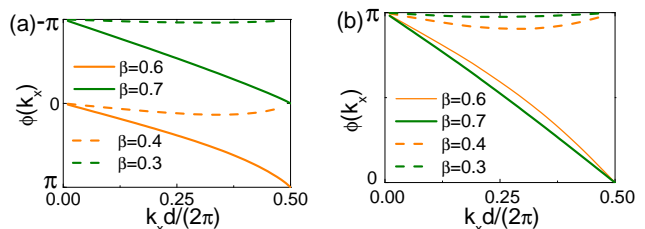


FIG. 2. The relative phase difference between p_A and p_B for momentum k_x , $\phi(k_x)$ for different dimerization parameters with (a) $d/\lambda_0 = 0.5$ and (b) $d/\lambda_0 = 0.2$.

The existence of nontrivial Zak phase $\gamma = \pi$ predicts topologically protected edge states at the boundary of the 1D dimerized chain. To show this property, we consider a finite dimerized chain with $N = 100$ identical atoms (50 dimers) with an open boundary. For finite chains, the band-structure can be determined numerically by calculating the eigenmodes through the coupled-dipole model of Eq. (1) under zero incident field for a finite chain [16, 21]. This equation specifies a set of solutions in the form $\tilde{\omega}_j = \omega_j - i\Gamma_j/2$ ($\Gamma_j > 0$) in the lower complex plane denoting to the eigenmodes of the dimerized chain (Note the $e^{-i\omega t}$ convention is assumed here). Here ω_j amounts to the frequency of an eigenmode while γ_j refers to its decay rate, where the corresponding eigenvector \mathbf{e}_j indicates the dipole excitation distribution of an eigenmode. We further analyze the inverse participation ratio (IPR)

from eigenvectors \mathbf{e}_j as [24]

$$IPR_j = \frac{\sum_{n=1}^N |\mathbf{e}_j(\mathbf{r}_n)|^4}{\left[\sum_{n=1}^N |\mathbf{e}_n(\mathbf{r}_n)|^2\right]^2}. \quad (5)$$

The IPR can be used to demonstrate the spatial confinement of different eigenmodes. For instance, for an IPR approaches $1/M$, where M is an integer, the corresponding eigenmode involves the excitation of M scatterers [24]. For a highly localized topological edge/interface mode, its IPR should be much larger compared to bulk modes [24].

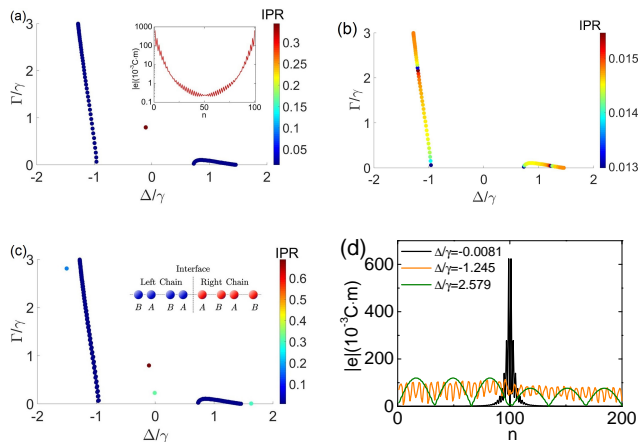


FIG. 3. (a) Eigenmode distribution for a dimerized chain with $N = 100$ atoms under $\beta = 0.6$ and $d/\lambda_0 = 0.5$. Note there are two edge states at ($\Delta/\gamma = -0.1056$, $\Gamma/\gamma = 0.7963$), and ($\Delta/\gamma = -0.1055$, $\Gamma/\gamma = 0.7960$). Inset: Dipole moment distribution (logarithmic scale) of an edge state (the same for both edge modes). (b) Eigenmodes of a topologically trivial dimerized chain with $N = 100$ atoms under $\beta = 0.4$ and $d/\lambda_0 = 0.5$. (c) Eigenmode distribution for a connected chain. Inset: Schematic of the connected chain. (d) Dipole moment distribution of the interface state at ($\Delta/\gamma = -0.0081$, $\Gamma/\gamma = 0.2258$) in (c), compared with those of bulk modes at ($\Delta/\gamma = -1.245$, $\Gamma/\gamma = 2.579$) and ($\Delta/\gamma = 1.453$, $\Gamma/\gamma = 6.3740 \times 10^{-4}$).

In Figs.3a and 3b, we show the eigenmode distributions for the cases of $\beta = 0.6$ and $\beta = 0.4$ with lattice period $d = 0.5\lambda_0$. In both cases we observe a bandgap is opened in the frequency range $-1 \lesssim \Delta/\gamma \lesssim 0.8$, which is consistent with the band-structure of an infinite chain. In the $\beta = 0.6$ case, we find two mid-gap states at $\Delta/\gamma = -0.1056$ and $\Delta/\gamma = -0.1055$. They both have a rather high IPR around 0.34. However, when $\beta = 0.4$ there are not any mid-gap states, and other bulk states exhibit very low IPRs. The mid-gap states are therefore topologically protected edge states, whose dipole moment distribution along the chain is shown in the inset of Fig.3a. This phenomenon is the direct outcome of the nontrivial band-structure for $\beta = 0.6$ as predicted by the Zak phase. Another feature of topological systems

is that, for two systems with different topological invariants, there exist topologically protected interface modes at the boundary of them. To demonstrate this property, in Fig.3c we calculate the eigenmode distribution for a connected chain, which comprises a topologically trivial chain with $\beta = 0.4$ in the left and a topologically nontrivial right chain with $\beta = 0.6$ in the right (inset of Fig.3c). It is observed that a highly subradiant interface mode emerges in the bandgap at $\Delta/\gamma = -0.0081$ with a decay rate of $\Gamma/\gamma = 0.2258$. Another midgap state is the edge state at the right boundary of the right chain. In Fig.3d we show the dipole moment distribution for the interface mode, compared with those of two bulk modes in the upper band ($\Delta/\gamma = 1.453$) and lower band ($\Delta/\gamma = -1.245$) respectively. The bulk modes periodically distributed in the left and right chains while the interface mode is highly localized.

In order to know how the mid-gap (edge) states of a dimerized chain evolve with the dimerization parameter, in Fig.4a we show the detuning and decay rate as a function of β for $d = 0.5\lambda_0$ and $d = 0.2\lambda_0$ respectively. It is observed that in both cases when the dimerization parameter increases from 0.5 to 1, the detunings of both edge states approach zero and their decay rates reach unity, leading to a behavior the same as the single-atom resonance. In fact, in dimerized plasmonic nanoparticle chains, it was found that the edge state frequency is the same as single-particle resonance frequency [6, 7, 16]. Thanks to the ultra-narrow linewidth of cold atoms, here we are able to observe the frequency shift of edge states from the single-atom resonance frequency, which is indeed substantial when d is small and β approaches 0.5. In Fig.4b, we also plot the bandgap width δ , which drastically expands when the dimerization increases, resulting in a 10000γ -wide gap for $\beta = 0.95$ under $d = 0.2\lambda$. Such a remarkable feature provides a very flexible platform for bandgap engineering in nanophotonic systems.

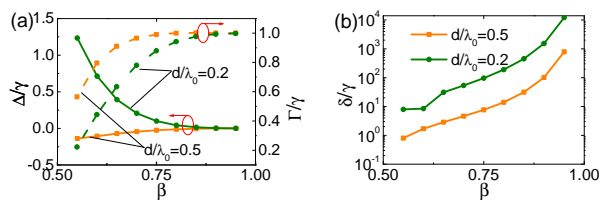


FIG. 4. (a) Edge mode frequency (detuning) Δ/γ and decay rate Γ/γ of topological nontrivial dimerized chain as a function of dimerization parameter β under $d/\lambda_0 = 0.5$ and $d/\lambda_0 = 0.2$. (b) Band gap size δ/γ as a function of dimerization parameter β under $d/\lambda_0 = 0.5$ and $d/\lambda_0 = 0.2$.

Finally, we focus on the $\beta = 0.6$, $d = 0.5\lambda_0$ dimerized chain and discuss the effects of disorder. Here disorder is introduced by shifting the positions of A atoms randomly in the range $[-\varepsilon d_1/2, \varepsilon d_1/2]$ along the x -axis, while the positions of B atoms are fixed, resulting a fixed period

d. In Figs.5a and 5b we give the eigenmode distributions for $\varepsilon = 0.1$ and $\varepsilon = 0.5$ respectively, which are both obtained after 100 random realizations. It is found that disorder can broaden the band-structure, leading to far-detuned states, especially for $\varepsilon = 0.5$. This is because under strong disorder, many atoms get very close to each other, leading to significant near-field dipole-dipole interactions and thus large frequency shifts [24]. In both weak-disorder and strong-disorder cases, topologically protected edge states with high IPRs still persist. Moreover, their IPRs mostly distribute in the range of [0.4, 0.85], which are even larger than that of the ordered dimerized chain ($IPR = 0.34$), indicating a stronger spatial confinement. In the inset of Fig.5a, the dipole moment distributions of the two edge states for a specific random realization are given for $\varepsilon = 0.1$. It is noted that different from the ordered case, these states in a disorder dimerized chain not only split in frequency domain substantially (not shown here), but also separate with each other in their dipole moment spatial distributions. The two identical two-sided edge modes in the ordered case evolve into two different one-sided edge modes in the disordered case. The same phenomenon is also observed for $\varepsilon = 0.5$. When $\varepsilon > 0.6$, we find that the edge modes start to mix with bulk modes and the band gap gets closed. However, in such high disorder, it is still possible to observe highly localized edge modes (not shown here).

In Fig.5c we calculate the eigenmode distribution of a connected chain which comprises a topologically non-trivial chain with $\beta = 0.6$ and disorder $\varepsilon = 0.5$ in the right, and a topologically trivial chain with $\beta = 0.4$ and disorder $\varepsilon = 0.5$ in the left, which is also obtained after 100 random realizations. In this circumstance, the topologically protected interface modes with high IPRs still persist in the gap near $\Delta/\gamma \sim 0$. In Fig.5d the dipole moment distribution for a typical interface mode is given. Remarkably, we find the dipole moment of at the interface is enhanced compared to that of the interface mode in the ordered case. We attribute this enhancement to the Anderson localization mechanism in strongly disordered systems. In Fig.5d we also show the edge mode in the right chain, which also resides in the gap, and a typical Anderson localized bulk mode, for a single random realization. It is found that the topologically protected edge and interface modes are more spatially localized than the Anderson localized mode, and result in stronger field enhancements.

In conclusion, we propose one-dimensional dimerized ultracold atomic chains as a realization for the SSH model. Topologically protected optical states are found at the edges of dimerized chains with nontrivial Zak phases, as well as at the interface between chains with different Zak phases. An analysis of the eigenmode distribution for finite chains demonstrates that such topological states exist in the bandgap and have very high IPRs. Furthermore, we show that such topological edge states

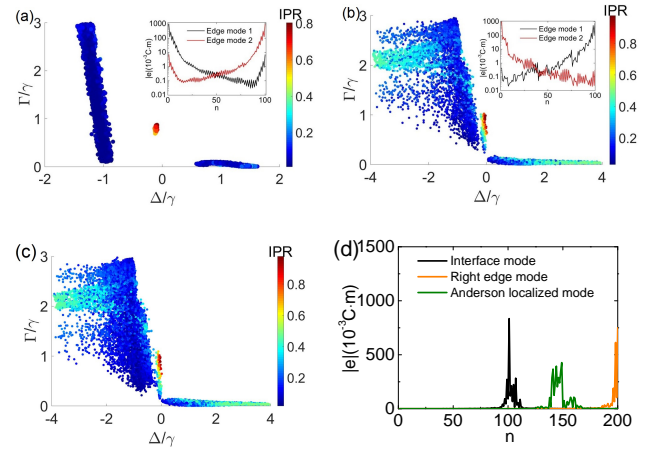


FIG. 5. (a) Eigenmode distribution for weakly disordered ($\varepsilon = 0.1$) dimerized chains with $N = 100$ atoms under $\beta = 0.6$ and $d/\lambda_0 = 0.5$. Results of 100 random realizations are shown. Inset: Dipole moment distributions (logarithmic scale) of the two edge states in a specific random configuration. (b) Eigenmode distribution for highly disordered ($\varepsilon = 0.5$) dimerized chains with $N = 100$ atoms under $\beta = 0.6$ and $d/\lambda_0 = 0.5$. Results of 100 random realizations are shown. Inset: Dipole moment distributions (logarithmic scale) of the two edge states in a specific random configuration. (c) Eigenmode distribution for connected dimerized chains comprising two disordered dimerized chains. Results of 100 random realizations are shown. (d) Dipole moment distributions of the interface state, as well as an edge state at the right boundary and an Anderson localized mode.

are robust under high-degree disorder and even enhanced by the disorder-induced Anderson localization. The ultra-strong scattering cross section and ultra-narrow linewidth of a single cold atom allows us to observe in more detail about topological states than conventional systems, such as the frequency shift with respect to the single-atom resonance and the largely tunable bandgap. We also expect that topological photonic modes in such dimerized ultracold atomic chains can provide an efficient interface for studying the topological states of light and matter [15]. Moreover, if nonlinear effects are included at high-intensity excitation, such dimerized chains can be applied to study the many-body physics of interacting photons [25, 26]. We also envisage some general features of topological photonic states in highly resonant point dipole systems, including quantum dots, plasmonic nanoparticles, etc., can be obtained from our study.

We thank the financial support from the National Natural Science Foundation of China (51636004, 51476097), Shanghai Key Fundamental Research Grant (16JC1403200), and the Foundation for Innovative Research Groups of the National Natural Science Foundation of China (51521004).

* changying.zhao@sjtu.edu.cn

- [1] L. Lu, J. D. Joannopoulos, and M. Soljačić, *Nature Photonics* **8**, 821 (2014).
- [2] A. B. Khanikaev and G. Shvets, *Nature Photonics* **11**, 763 (2017).
- [3] C. Poli, M. Bellec, U. Kuhl, F. Mortessagne, and H. Schomerus, *Nature communications* **6**, 6710 (2015).
- [4] R. El-Ganainy and M. Levy, *Opt. Lett.* **40**, 5275 (2015).
- [5] M. Parto, S. Wittek, H. Hodaei, G. Harari, M. A. Bandres, J. Ren, M. C. Rechtsman, M. Segev, D. N. Christodoulides, and M. Khajavikhan, *Phys. Rev. Lett.* **120**, 113901 (2018).
- [6] C. W. Ling, M. Xiao, C. T. Chan, S. F. Yu, and K. H. Fung, *Opt. Express* **23**, 2021 (2015).
- [7] C. A. Downing and G. Weick, *Phys. Rev. B* **95**, 125426 (2017).
- [8] A. Blanco-Redondo, I. Andonegui, M. J. Collins, G. Harari, Y. Lumer, M. C. Rechtsman, B. J. Eggleton, and M. Segev, *Phys. Rev. Lett.* **116**, 163901 (2016).
- [9] A. P. Slobozhanyuk, A. N. Poddubny, A. E. Miroschnichenko, P. A. Belov, and Y. S. Kivshar, *Phys. Rev. Lett.* **114**, 123901 (2015).
- [10] S. Longhi, *Opt. Lett.* **38**, 3716 (2013).
- [11] I. Bloch, *Nature Physics* **1**, 23 (2005).
- [12] M. Endres, H. Bernien, A. Keesling, H. Levine, E. R. Anschuetz, A. Krajenbrink, C. Senko, V. Vuletic, M. Greiner, and M. D. Lukin, *Science*, aah3752 (2016).
- [13] D. Barredo, S. De Léséleuc, V. Lienhard, T. Lahaye, and A. Browaeys, *Science* **354**, 1021 (2016).
- [14] B. J. Lester, N. Luick, A. M. Kaufman, C. M. Reynolds, and C. A. Regal, *Physical review letters* **115**, 073003 (2015).
- [15] N. Goldman, J. Budich, and P. Zoller, *Nature Physics* **12**, 639 (2016).
- [16] S. R. Poccok, P. A. Huidobro, and V. Giannini, arXiv preprint arXiv:1710.09782 (2017).
- [17] B. Olmos, D. Yu, Y. Singh, F. Schreck, K. Bongs, and I. Lesanovsky, *Phys. Rev. Lett.* **110**, 143602 (2013).
- [18] A. A. Svidzinsky, J.-T. Chang, and M. O. Scully, *Phys. Rev. A* **81**, 053821 (2010).
- [19] W. Guerin, M. O. Araújo, and R. Kaiser, *Phys. Rev. Lett.* **116**, 083601 (2016).
- [20] J. Javanainen and J. Ruostekoski, *Opt. Express* **24**, 993 (2016).
- [21] W. H. Weber and G. W. Ford, *Phys. Rev. B* **70**, 125429 (2004).
- [22] B. X. Wang, C. Y. Zhao, Y. H. Kan, and T. C. Huang, *Opt. Express* **25**, 18760 (2017).
- [23] J. Zak, *Phys. Rev. Lett.* **62**, 2747 (1989).
- [24] R. Wang, M. Rontgen, C. V. Morfonios, F. A. Pinheiro, P. Schmelcher, and L. D. Negro, arXiv preprint arXiv:1801.03550 (2018).
- [25] E. Shahmoon, D. S. Wild, M. D. Lukin, and S. F. Yelin, *Phys. Rev. Lett.* **118**, 113601 (2017).
- [26] J. Perczel, J. Borregaard, D. E. Chang, H. Pichler, S. F. Yelin, P. Zoller, and M. D. Lukin, *Phys. Rev. Lett.* **119**, 023603 (2017).